ChemPubSoc Europe

DOI: 10.1002/ejic.201900745

EurJIC European Journal of Inorganic Chemistry

Full Paper

Metal Oxoclusters

Hybrid EUV Resists with Mixed Organic Shells: A Simple Preparation Method

Lianjia Wu,[a] Jeremy Liu,[a] Michaela Vockenhuber,[b] Yasin Ekinci,[b] and Sonia Castellanos*[a]

Abstract: Metal-containing molecular hybrid compounds, such as metal oxoclusters (MOCs), are promising materials for extreme ultraviolet (EUV) lithography. The solubility, processability, and reactivity towards EUV photons in these compounds are mostly determined by the composition of their organic shells. Therefore, gaining molecular control on the composition of the shell is crucial to tune their lithographic performance of sensitivity, resolution, and line-edge roughness. In this work, a new method to prepare MOCs that feature two types of carboxylate ligands is presented. In this method, amine-functionalized resins are used for the purification step. By using this protocol, Ti- and Zr-based MOCs with mixed-ligands organic shells were synthesized. The new compounds showed clear differences in the processability and sensitivity as EUV resists compared to their analogues featuring only one type of ligand. The results validate this new synthetic approach for the preparation of custom-made EUV resists towards better lithographic performance.

Introduction

The roadmap of the semiconductor industry demands the continuous miniaturization of the electronic components in computer chips. To fulfil this goal, a new nanolithography technology is introduced into the market: extreme ultraviolet lithography (EUVL).[1–3] This technique evolved from the traditional optical photolithography, where a pattern is written with light shining on a photosensitive material known as photoresist. The illuminated areas undergo photochemical reactions that lead to changes in the solubility properties of the material. This allows for the selective dissolution of either the exposed or the unexposed areas with a suitable developer. One of the main differences of EUVL with respect to previous generations of photolithography is the wavelength used for the pattern projection. EUVL employs 13.5 nm in order to overcome the resolution limits of the deep UV technology, which employs 193 nm wavelength. The main consequence is that absorption of light in this energy regime (soft X-ray) leads to photoionization instead of resonant electronic transitions and, therefore, the chemical reactions are mainly performed by the secondary electrons generated upon irradiation. In addition, the probability of absorption of EUV photons is mainly determined by the elemental composition of the photoresist,[4,5] rather than the selection rules of classical photochemistry, where the characteristics of the frontier molecular orbitals can be used to predict the absorption probability.

Since conventional photoresists based on light elements exhibit low EUV absorptivity, new photoresist materials that incorporate elements with high EUV photon absorption cross-section, such as metallic elements, are attracting much interest in the EUVL field.[3,6] Yet, while the inorganic elements in these materials are considered responsible for the photon capture, the mechanism that leads to the solubility change is mainly determined by the reactivity of their organic components.[7,8]

Metal oxoclusters (MOCs) are molecular hybrid compounds with inorganic core-organic shell structures,[9,10] which are ideal platforms as EUV photoresist.[7,11] They have well-defined inorganic cores and organic shells and, as a result of their molecular nature, they are small and have homogeneous (monodisperse) sizes by definition. These aspects contribute to the reduction of stochastic sources that are partly responsible for the "noise" in the nanopatterns, that is, irregularities in the features' edges (measured as line-edge roughness) and/or widths (measured as line-width roughness).[12]

In a recent work, we showed that Zr-based metal oxoclusters featuring methacrylate ligands are promising EUV photoresists (Scheme 1).[7] This material is comprised of an hexametalic oxo-core and twelve ligands in bridging and chelating coordination modes[13] ($Zr_6O_4(OH)_4Mc_{12}$ noted as Zr_6Mc_{12} in this paper). The change in solubility that this material undergoes upon EUV irradiation mainly originates from the cross-linking of the methacrylate ligands. Yet, the lithographic performance of Ti-based oxoclusters could not be tested due to the poor solubility of this material, which hindered its deposition as a thin film.[14]

[a] *Advanced Research Center for Nanolithography, Science Park 106, 1098XG Amsterdam, The Netherlands*
https://arcnl.nl/research-groups/euv-photoresists
E-mail: s.castellanos@arcnl.nl
https://twitter.com/nanolithography
[b] *Paul Scherrer Institute, 5232 Villigen, Switzerland*

Supporting information and ORCID(s) from the author(s) for this article are available on the WWW under https://doi.org/10.1002/ejic.201900745.

This compound consists of an octameric ring of metal atoms bridged by μ_2-O oxygens and 16 methacrylate ligands ($Ti_8O_8Mc_{16}$ noted as Ti_8Mc_{16}).[15]

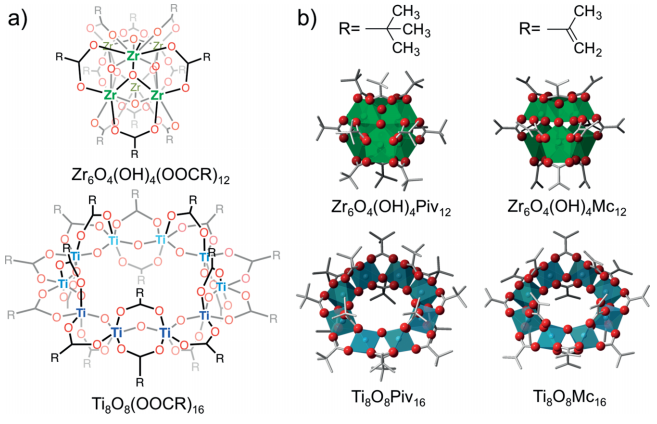

Scheme 1. a) General molecular formulae of the hexameric Zr-based and the octameric Ti-based oxoclusters with carboxylate ligands. b) Molecular structure of the clusters as resolved from X-ray crystalline diffraction.[13,15–17] The coloured polyhedra represent the coordination geometry of the metal, the red spheres the oxygen atoms and the grey bars the carbon backbone of the pivalate or methacrylate ligands.

The analogous material featuring pivalate ligands (Ti_8Piv_{16})[16,18] renders better solubility in organic solvents like chloroform, toluene, and tetrahydrofuran. However, the films obtained by spin-coating are of bad quality due to their poor wettability on the Si-substrate, even when the Si surface is functionalized to be hydrophobic.

A characteristic of MOCs that makes them particularly interesting as EUV photoresists is their synthetic versatility. The latter arises from the dynamic bonding between the metals in the oxocore and the carboxylate ligands in the shell, which allows for easy exchange of the organic ligands[16,19–22] and thus a simple way of modifying their composition. This offers a much advantageous tool to study the chemistry that different functionalities can undergo upon EUV irradiation and investigate their impact on the lithographic performance of the material.[23,24] Such need of fundamental understanding on the EUV-induced chemistry is a pressing issue in the field of EUV lithography, since the success of this new technology is partly depending on the sensitivity, resolution limit, and defect density that the photoresist material can yield in the patterning process.

Despite the simplicity of ligand exchange reactions between ligands that have the same coordination geometries (binding multiplicity and angle), the isolation and purification of the resulting oxoclusters with mixed shells is not straightforward. The most common method of isolation of metal oxoclusters is crystallization.[16,20] However, purification of metal oxoclusters designed for lithographic applications by means of crystallization is not optimal for two main reasons. First, as part of the lithographic process, the material must be deposited as homogeneous thin films of a few nanometers of thickness (20–30 nm) using spin-coating. This means that the metal oxoclusters must be soluble in organic solvents and able to provide homogeneous amorphous films. Yet, structural characteristics that enhance solubility and amorphous solid phases typically do not favour packing in crystalline arrangements. Second, as explained above, it is highly desired that several functionalities can be incorporated simultaneously in the metal oxoclusters (mixed-shell) so that the chemistry that yields the solubility change of the material can be finely tuned. However, crystallization becomes extremely challenging when a distribution of oxocluster molecules with mixed-shell compositions is formed during ligand exchange reaction. In fact, to the best of our knowledge, isolation of oxoclusters resulting from ligand exchange on the Zr_6 and Ti_8 oxocores by crystallization has only been reported for fully exchanged organic shells,[16] whereas oxoclusters with mixed-shells could only be isolated by crystallization when crystals are formed during the condensation reaction between the metal alkoxide precursor and a mixture of carboxylic acids.[20] Furthermore, in the latter case, accessing all ratios of the two ligands would require a broad screening of reaction conditions.

In this work, we conceived a preparation method of mixed-shell Zr- and Ti-metal oxoclusters based on a purification step with resins functionalized with basic amine groups. Having two different ligands in the organic shell of these compounds had two main purposes. In the case of Ti-MOCs, we aimed at introducing ligands that facilitate their dissolution together with ligands that favour the formation of thin films and also enable the cross-linking reaction as a means for patterning. In the case of Zr-MOCs, the mixed-ligand shell enables studying the effect of decreasing the number of terminal double bonds in the organic shell. Once the mixed-shell were attained by ligand exchange reactions, the basic resins were used to extract the excess of carboxylic acids. This method allows for the easy preparation of metal oxoclusters with complex organic shell composition and proves to be a good synthetic tool that allows modulating the EUV sensitivity of this type of materials by tuning their molecular structure.

Results and Discussion

Resins that are functionalized with tertiary amines have been used in the past to remove carboxylic acids from organic solvents.[25,26] In the present work, the resins that were selected for the purification step after ligand exchange reaction were polystyrene (PS) resins functionalized with tertiary amines, PS-*N*-piperidine (in this work PIP) and PS-*N*-dimethylamine (in this work DMA). Bulky amines were chosen to avoid any competition with the carboxylate ligand in the coordination with the metals of the MOC inorganic core. The affinity of these two basic resins towards five different carboxylic acids (pivalic, methacrylic, propionic, butyric, and isobutyric acid) that are of interest to enhance solubility properties and film formation capability of MOCs was evaluated by means of ^{1}H NMR. To do so, the change of concentration of the acid in a solution of deuterated chloroform after adding the corresponding resin (1:1 molar ratio of amine on resin/acid) was used to calculate the equilibrium adsorption, q_e,[27,28] as:

$$q_e = (c_0 - c_e)/m \times V$$

where c_0 and c_e are the initial concentration and the concentration in equilibrium in mg/L, m is the mass of resin in g and V is the volume of the suspension in L (Figure 1).

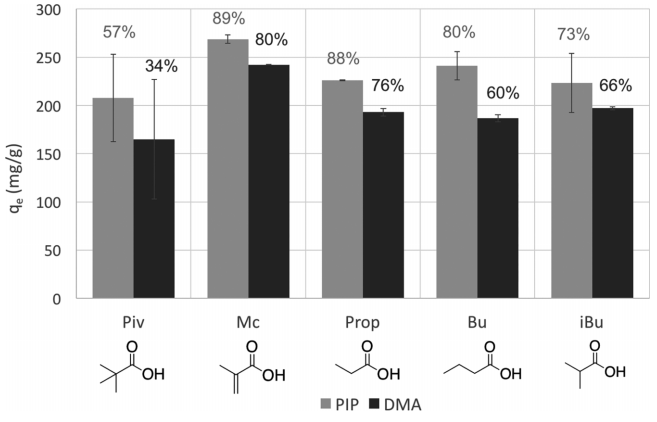

Figure 1. Equilibrium adsorption (q_e) measured for dimethylaminomethyl- (DMA) and piperidine-functionalized (PIP) resins and five different carboxylic acids. The percent of acid absorbed by each resin is indicated on top of the bar. All reactions were performed using a 1:1 molar ratio of amine on the resin to carboxylic acid.

In all cases, the resin functionalized with piperidine showed stronger affinity towards all carboxylic acids and in particular towards methacrylic acid. On the other hand, the carboxylic acid with the bulkier backbone, pivalic acid (Piv), appeared to adsorb more poorly on both resins.

The use of resins for the purification process was first tested on Ti-oxoclusters in small scale and monitored by ^{1}H NMR. Ti_8Piv_{16} was used as starting material and ligand exchange reactions with different molar ratios of MOC to methacrylic acid (1:16 and 1:20) were performed on this compound in deuterated chloroform. After that, the resulting solution was treated with basic resin, the resin was filtered out, and the composition of the filtered solution was newly determined (Figure 2). This last step was realised twice to monitor how the second cycle of resin treatment could further remove the free carboxylic acids.

The chelation dynamics of the carboxylate ligands on this metallic cluster are slow enough at room temperature to allow to distinguish the protons of ligands that are bonded to the metals from the ones of the acids that are non-bonded and free in the deuterated chloroform solution (Table 1). The average ratio of pivalate/methacrylate ligand in the Ti-MOC that resulted from these exchange reactions was calculated from the peak areas in the ^{1}H NMR spectra (Figure 3).

When stoichiometric amounts of methacrylic acid were added to Ti_8Piv_{16}, an oxocluster with almost 1:1 ratio of methacrylate/pivalate ligands was obtained, i.e. $Ti_8Piv_8Mc_8$. The average amount of methacrylate ligands in the shell was increased by increasing the molar ratio of methacrylate acid in the reaction mixture (Figure 3, white columns). After treating the mixtures with each basic resin (DMA and PIP) in a 1:1 carboxylic acid/amine molar ratio (amine concentration estimated from the nitrogen content specified by the commercial provider), the percent of non-coordinated carboxylic acids decreased from 50 % to 14 % in the 1:16 MOC/methacrylic reaction, and from 55 % to 10 % in the 1:20 reaction after two resin treatment

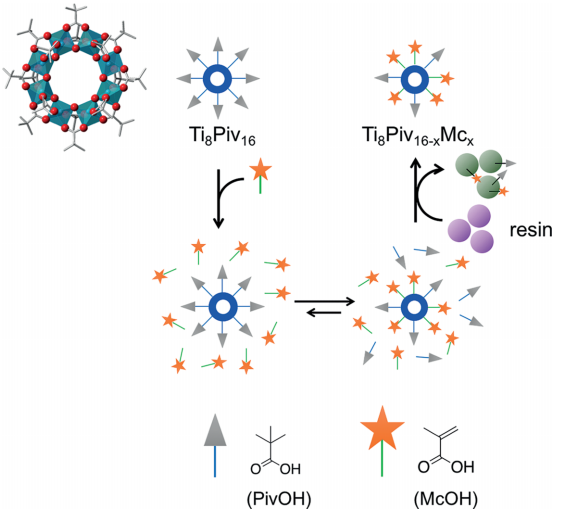

Figure 2. Scheme showing the steps of the new protocol for the preparation of mixed-ligand metal oxoclusters. The pristine oxocluster with pivalate ligands Ti_8Piv_{16} is dissolved in a solution with methacrylic acid and ligand exchange occurs. The amine-functionalized resin is added and the non-coordinated carboxylic acids are adsorbed on it and removed by filtration.

Table 1. ^{1}H NMR chemical shifts of carboxylic acids and carboxylate ligands in the solution mixture of the ligand exchange reactions of Ti-oxoclusters in $CDCl_3$.

^{1}H NMR chemical shifts [ppm]		Free acid	Coordinated ligand
Pivalic acid/pivalate	$-CH_3$	1.24	1.16, 1.19
Methacrylic acid/ Methacrylate	$-CH_3$	1.95	1.86, 1.92
	$=CH_2$	5.68, 6.24	5.49, 5.55, 6.19, 6.21

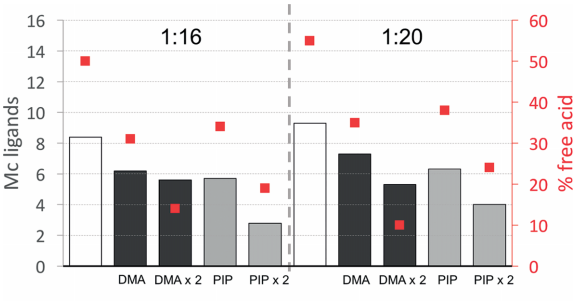

Figure 3. Columns: number of methacrylate ligands (x) incorporated in $Ti_8Piv_{16-x}Mc_x$ after ligand exchange reaction (white) and after treatment with one or two cycles (× 2) of DMA (black) or PIP (grey) resins. Red squares: percent of free acid in the solution over the total amount of carboxylate ligands and carboxylic acids.

cycles (red squares in Figure 3). However, the ratio of the methacrylate ligand in the oxocluster also decreased. This effect is stronger in the case of the PIP resin which made the content of methacrylate ligands in the MOC shell decrease from 8 to a minimum of 3 (1:16 ratio) and from 9 to a minimum of 4 (1:20 ratio) after the resins treatment. The results are in line with the higher affinity of both resins towards methacrylic acid compared to pivalic acid previously observed. Nevertheless, in all cases, Ti-MOCs with a binary composition in the organic shell and a reduced amount of free acids were obtained.

The approach was scaled up and utilised to prepare Ti-based MOCs and Zr-based MOCs with mixed shells that contain both methacrylate and pivalate ligands. Dimethylamine-resin was used since it reverted the introduction of methacrylate to a less extent than the piperidine-resin (Scheme 2).

$$Ti_8Piv_{16} + 16\ McOH \xrightarrow{DMA\ resin} Ti_8Piv_{10}Mc_6$$

$$Zr_6Piv_{12} + 36\ McOH \xrightarrow{DMA\ resin} Zr_6Piv_4Mc_8$$

Scheme 2. Ligand exchange reactions followed by resin purification.

For the reaction with Ti_8Piv_{16}, a 1:16 MOC/acid molar ratio was employed, in order to compare with the small scale NMR experiments. In this experiment, the solution treated with DMA-resin (one cycle only) yielded the same ratio observed in the NMR experiment (Piv/Mc, 10:6). Yet, the number of free acids was even lower than the one detected in the NMR studies (ca. 18 % of free acid) thus yielding a product with an average formula of $Ti_8Piv_{10}Mc_6$•2PivOH•1McOH. We assume that the evaporation of the solvent at reduced pressure after the resins treatment contributed to reducing the amount of free acid. Characterization of this compound by IR spectroscopy (Figure 4) displayed a mixture of characteristic peaks of the MOCs with pure pivalate (Ti_8Piv_{16}) and pure methacrylate (Ti_8Mc_{16}) shells (Figure 4). In addition, peaks associated with the non-coordinated free carboxylic acid (C=O stretching at 1700 cm^{-1} and broadband corresponding to O-H stretching in the 2400–3600 cm^{-1} range) were also present.

In the case of the Zr-based cluster, our aim was to investigate how the incorporation of a small number of pivalate ligands in a methacrylate rich organic shell would affect the cross-linking mechanism induced by EUV light compared to previously studied Zr_6Mc_{12} photoresist. For this reason, a higher ratio of methacrylic acid was used for the ligand exchange reaction on Zr_6Piv_{12} and the resin treatment was applied only in one cycle. In contrast to the case of the Ti-based pivalate oxoclusters, the Zr_6Piv_{12} cluster is originally not soluble in chloroform. However, when this compound is suspended in chloroform in the presence of methacrylic acid, the incorporation of the methacrylate ligands in the clusters by means of ligand exchange reactions leads to the dissolution of the mixed-shell compound. The ^1H NMR spectrum after the reaction revealed that a cluster with a 4:8 Piv/Mc ratio was obtained (see Supporting Information). Yet, the dynamics of exchange between free acids and bonded acid are too fast to determine the content of free acid for this product by ^1H NMR. Nevertheless, and as in the case of the Ti-based counterpart, the IR displayed peaks characteristic for Zr_6Piv_{12} and Zr_6Mc_{12} (synthesized according to the literature) as well as the presence of free acids by the broad O-H stretching band and the C=O stretching peak, as in the Ti-MOC (Figure 4). The average composition of the final product is thus estimated as $Zr_6Piv_4Mc_8$ from NMR experiments.

The isolated products $Ti_8Piv_{10}Mc_6$ and $Zr_6Piv_4Mc_8$ were tested as EUV photoresists. The first noticeable effect of providing the Ti-oxocluster with a mixed organic shell was that it enabled its deposition as a thin film from solution by spin-coating, in contrast to the case of the analogous compounds with only pivalate or only methacrylate ligands. The sensitivity to extreme ultraviolet light of the materials was evaluated using synchrotron radiation at the EUV interference lithography tool (XIL-II) at Paul Scherrer Institute (PSI).[29] This property is defined as the minimum dose of EUV light necessary to induce a chemical

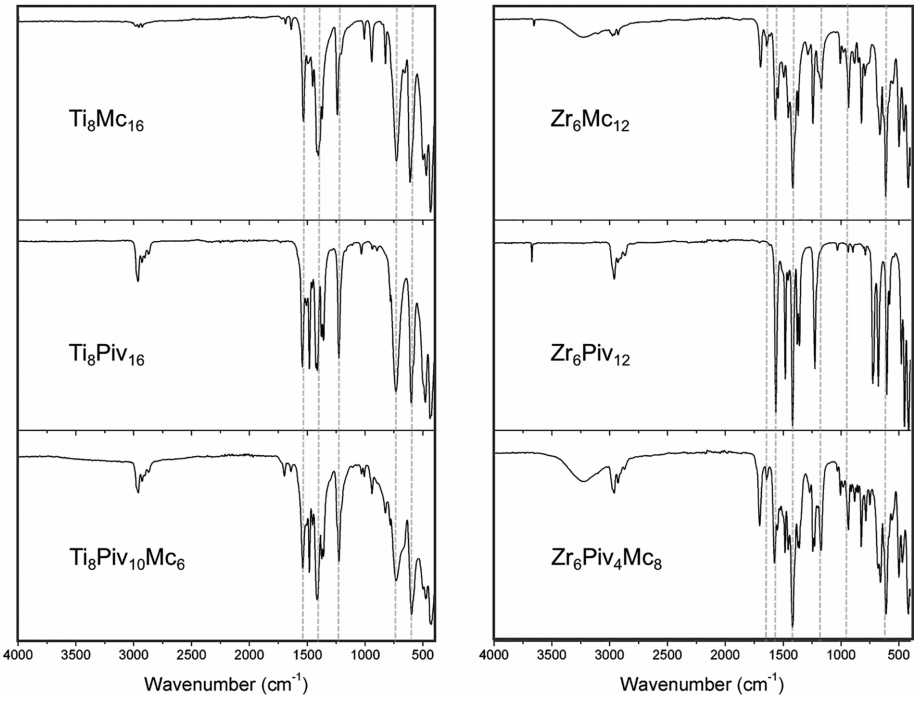

Figure 4. IR spectra of the products of the scaled-up ligand exchange reactions after treatment with DMA and isolation of the cluster as a powder by means of reduced pressure solvent evaporation.

change that leads to a change in the solubility of the compound and is determined by means of a contrast curve. That is, the extent of the chemical changes induced by EUV light can be indirectly measured by the differences in solubility rate of the material in a specific solvent as a function of dose. For negative tone resists, such as the ones studied in the present work, the solubility rate decreases with the EUV exposure dose. Therefore, the amount of material left on the substrate, measured as thickness, for a given development time increases with the dose, which yields the aforementioned contrast curve plot (Figure 5).

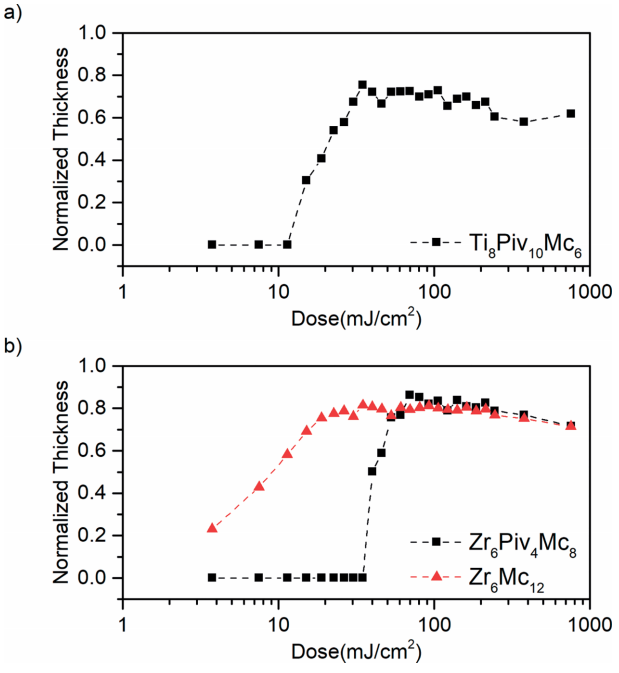

Figure 5. Contrast curves of (a) $Ti_8Piv_{10}Mc_6$ (original thickness d_0 = 17 nm) using toluene for development, (b) Zr_6Mc_{12} (d_0 = 24 nm), and $Zr_6Piv_4Mc_8$ (d_0 = 24 nm) using chloroform as the developer.

Our experiments showed that the Ti-oxocluster with mixed-ligand organic shell $Ti_8Piv_{10}Mc_6$ acted as a negative-tone EUV photoresist when toluene was used as developer (Figure 5a). In the case of the Zr-oxocluster, chloroform was used as developer to compare with previous results obtained for the analogous material with only methacrylate ligands Zr_6Mc_{12}. It was observed that the sensitivity of the mixed-sell compound $Zr_6Piv_4Mc_8$ was lower than the one of Zr_6Mc_{12}, that is, a higher dose is required to induce a solubility switch in the mixed-shell oxocluster. This observation is in agreement with the lower number of cross-linkable terminal double bonds of $Zr_6Piv_4Mc_8$ compared to the previously studied Zr_6Mc_{12}. That is, the radiation-induced cross-linking of terminal double bonds is less likely to occur in clusters with a lower ratio of methacrylate ligands. Therefore, the extent of chemical change that leads to a change in solubility rate requires more photons in the case of the mixed-ligand cluster.

Conclusions

Metal oxoclusters based on Ti and Zr featuring mixed carboxylate organic shells can be easily prepared and isolated by means of ligand exchange reactions followed by a basic resin treatment to remove the exceeding acid molecules. These methods allow incorporating two types of carboxylate ligands in different ratios avoiding a crystallization step. This protocol proved to be a useful tool for the modification of the lithographic performance of metal oxoclusters that act as extreme ultraviolet photoresist. In particular, the introduction of pivalate and methacrylate ligands in Ti-octamer ($Ti_8Piv_{10}Mc_6$) enables its deposition in thin films and its utilization as negative tone resist. On the other hand, the presence of these two ligands in Zr-hexamer oxoclusters ($Zr_6Piv_4Mc_8$) led to the decrease in sensitivity of the material compared to the parent compound with only methacrylate ligands. This result is in line with the lower number of terminal units that can cross-link upon light exposure, which yields slower cross-linking kinetics and thus require higher photon doses for a full transformation into an insoluble network. Our work proves that the processability and the reactivity of this type of materials can be finely tuned by means of this new synthetic protocol and thus offers a versatile tool for the preparation of future extreme ultraviolet resist materials for nanolithography applications.

Experimental Section

Polystyrene-resins functionalized with tertiary amines were purchased from Sigma-Aldrich (dimethylaminomethyl-polystyrene, catalogue number 39205; piperydine, polymer-bound, catalogue number, 49,461–5).

Ti_8Piv_{16} was synthesized as described in reference.[19] Zr_6Piv_{12} was prepared with an analogous method. Pivalic acid (2 g, 20 mmol) was added to a solution of zirconium isopropoxide in 2-propanol 70 % (1 mL, 2.28 mmol). The mixture was placed in an autoclave and heated up at 80 °C for 24 h. The reaction gave white crystals that were filtered off and washed with diethyl ether to give the insoluble cluster Zr_6Piv_{12} (540 mg, 76 %), as identified from powder X-ray diffraction (Figure S1 in Supporting information) and IR, which gave identical features as compared to the ones reported in the literature for the same compound.[17] Thermogravimetric analysis (TGA) was also in agreement with the expected composition (calculated ZrO_2 residue 39 %, found 32 %, Figure S4 in Supporting Information)

^{1}H NMR experiments were performed in a Bruker Avance 300 MHz spectrometer, FTIR-ATR experiments of bulk samples were performed in a Bruker ALPHA-II FTIR spectrometer. FTIR spectra of spin-coated thin films were recorded with a Bruker Vertex 80v spectrometer. TGA was performed using NETZSCH thermogravimetric analyzer in an Al_2O_3 crucible and heating was performed from 35 °C to 800 °C at 10 K/min in an 80:20 N_2/O_2 atmosphere. The thickness measurements were performed using a Bruker atomic force microscopy (AFM) with the ScanAsyst mode.

Equilibrium adsorption of resins. To the carboxylic acid (0.1 mmol) in deuterated chloroform (1 mL) solution was added the piperidine- or dimethylaminomethyl-functionalized resin (0.1 mmol of amine content estimated from N content according to the supplier). The solution was stirred for 30 min. Then, the resin was filtered out of the solution. To 0.75 mL of the solution, toluene or pyridine (10 μL) was added as a standard for quantification of acid left in solution by ^{1}H-NMR (300 MHz) measurement.

Determination of ligand ratio after ligand exchange reaction and purification with resin. Ti_8Piv_{16} (10 mg) were dissolved in $CDCl_3$

(1 mL) and the carboxylic ligand was added in molar ratios of 1:12, 1:16, 1:20 or 1:36. The reaction mixture was stirred for 30 min. A resin was added to the reaction in a 1:1 molar ratio of carboxylic acid/amine in resin (based on N content of the resin) and the mixture was stirred for 30 min. The solution was filtered and analyzed by ^{1}H-NMR. The composition of the organic shell was determined by the signal ratio between the bonded ligands.

Scaled-up synthesis of $Ti_8Piv_{10}Mc_6$ and $Zr_6Piv_4Mc_8$. Ti_8Piv_{16} and Zr_6Piv_{12} (300 mg) were dissolved or suspended in chloroform (20 mL) respectively. Methacrylic acid was added in molar ratios of 1:16 or 1:36. The reaction mixture was stirred for 30 min. Resin was added in a ratio of amine to carboxylic ligand ratio of 1:1 (based on N content of the resin) and the reaction mixture was stirred for 30 min. The resin was filtered out and the solvent was evaporated. The product was analyzed with ^{1}H-NMR and IR spectrometer.

Spin coating of mixed-ligand MOCs. $Ti_8Piv_{10}Mc_6$ or $Zr_6Piv_4Mc_8$ was dissolved in toluene (10 mg/mL). The solution was filtered with a 0.2 um filter and deposited on a silicon substrate by spin-coating (2400 rpm, 30 s, 2000 rpm/s acceleration for $Ti_8Piv_{10}Mc_6$ and 3000 rpm/s for $Zr_6Piv_4Mc_8$).

Exposure in XIL-II. EUV open-frame exposure was performed at the XIL-II beamline of Swiss Light Source (SLS) at the PSI. Doses were varied from 3.75 to 756 mJ/cm^2. Toluene and chloroform were tested as developers for exposed photoresists for 20 s and 15 s respectively.

Acknowledgments

We acknowledge the Paul Scherrer Institute, Villigen, Switzerland for the provision of beamtime at beamline XIL-II of the SLS (20180993). The research leading to these results has received funding from the European Community's Seventh Framework Programme (FP7/2007-2013) under grant agreement n.°312284 (CALIPSO, 20180993).

Keywords: Inorganic-Organic hybrid composites · Zirconium · Titanium · EUV lithography · Ligand exchange

[1] A. Robinson, R. Lawson, in *Frontiers of Nanoscience* (Ed.: R. E. Palmer), Elsevier, **2016**.
[2] P. D. Ashby, D. L. Olynick, D. F. Ogletree, P. P. Naulleau, *Adv. Mater.* **2015**, *27*, 5813–5819.
[3] L. Li, X. Liu, S. Pal, S. Wang, C. K. Ober, E. P. Giannelis, *Chem. Soc. Rev.* **2017**, *46*, 4855–4866.
[4] R. Fallica, J. Haitjema, L. Wu, S. Castellanos, A. M. Brouwer, Y. Ekinci, *J. Micro/Nanolitho. MEMS MOEMS* **2018**, *17*, 23505.
[5] R. Fallica, J. K. Stowers, A. Grenville, A. Frommhold, A. P. G. Robinson, Y. Ekinci, *Proc. SPIE* **2016**, *9776*, 977612.
[6] H. Xu, V. Kosma, K. Sakai, E. P. Giannelis, C. K. Ober, *J. Micro/Nanolitho. MEMS MOEMS* **2018**, *18*, 1.
[7] L. Wu, M. Baljozovic, G. Portale, M. Vockenhuber, T. Jung, Y. Ekinci, S. Castellanos, *J. Micro/Nanolitho. MEMS MOEMS* **2019**, *18*, 13504.
[8] E. C. Mattson, Y. Cabrera, S. M. Rupich, Y. Wang, K. A. Oyekan, T. J. Mustard, M. D. Halls, H. A. Bechtel, M. C. Martin, Y. J. Chabal, *Chem. Mater.* **2018**, *30*, 6192–6206.
[9] U. Schubert, *Coord. Chem. Rev.* **2017**, *350*, 61–67.
[10] U. Schubert, *Chem. Soc. Rev.* **2011**, *40*, 575–582.
[11] H. Xu, K. Sakai, K. Kasahara, V. Kosma, K. Yang, H. C. Herbol, J. Odent, P. Clancy, E. P. Giannelis, C. K. Ober, *Chem. Mater.* **2018**, *30*, 4124–4133.
[12] R. Maas, M. Van Lare, S. F. Wuister, R. Maas, M. Van Lare, G. Rispens, S. F. Wuister, *J. Micro/Nanolitho. MEMS MOEMS* **2018**, *17*, 41003.
[13] G. Kickelbick, U. Schubert, *Chem. Ber. Recl.* **1997**, *130*, 473–478.
[14] S. Castellanos, L. Wu, M. Baljozovic, G. Portale, D. Kazazis, M. Vockenhuber, Y. Ekinci, T. Jung, *Proc. SPIE* **2018**, *10583*, 105830A.
[15] C. Artner, M. Czakler, U. Schubert, *Chem. Eur. J.* **2014**, *20*, 493–498.
[16] T. Frot, S. Cochet, G. Laurent, C. Sassoye, M. Popall, C. Sanchez, L. Rozes, *Eur. J. Inorg. Chem.* **2010**, 5650–5659.
[17] P. Piszczek, A. Radtke, A. Grodzicki, A. Wojtczak, J. Chojnacki, *Polyhedron* **2007**, *26*, 679–685.
[18] P. Piszczek, M. Richert, A. Grodzicki, T. Głowiak, A. Wojtczak, *Polyhedron* **2005**, *24*, 663–670.
[19] C. H. Hendon, D. Tiana, M. Fontecave, C. Sanchez, L. D'Arras, C. Sassoye, L. Rozes, C. Mellot-Draznieks, A. Walsh, *J. Am. Chem. Soc.* **2013**, *135*, 10942–10945.
[20] F. R. Kogler, M. Jupa, M. Puchberger, U. Schubert, *J. Mater. Chem.* **2004**, *14*, 3133–3138.
[21] J. Kreutzer, M. Puchberger, C. Artner, U. Schubert, *Eur. J. Inorg. Chem.* **2015**, *2015*, 2145–2151.
[22] V. Guillerm, S. Gross, C. Serre, T. Devic, M. Bauer, G. Férey, *Chem. Commun.* **2010**, *46*, 767–769.
[23] L. Wu, M. Vockenhuber, Y. Ekinci, S. Castellanos, *Proc. SPIE* **2019**, *10957*, 10957B.
[24] L. Wu, M. Tiekink, A. Giuliani, L. Nahon, S. Castellanos, *J. Mater. Chem. C* **2019**, *7*, 33.
[25] B. C. Bookser, S. Zhu, *J. Comb. Chem.* **2001**, *3*, 205–215.
[26] H. M. Anasthas, V. G. Gaikar, *React. Funct. Polym.* **2001**, *47*, 23–35.
[27] H. Uslu, S. Majumder, *J. Chem. Eng. Data* **2017**, *62*, 1501–1506.
[28] S. Kumar, S. Batra, D. Datta, *J. Mol. Liq.* **2017**, *247*, 289–293.
[29] N. Mojarad, J. Gobrecht, Y. Ekinci, *Microelectron. Eng.* **2015**, *143*, 55–63.

Received: July 8, 2019